Modeling and Simulation of Copper Removal from the Contaminated Soil by a Combination of Adsorption and Electro-kinetic Remediation

Ass. Prof. Dr. Ayad Abed Al-hamza Faisal
Eng., College, Dept. of Envir. Eng.
Baghdad University
E-mail: ayadabedalhamzafaisal@yahoo.com

Ahmed Alaa Hussein
Eng., College, Dept. of Envir. Eng.
Al-Mustansiriyah University
E-mail: malakaz08@yahoo.com

ABSTRACT

Electro-kinetic remediation technology is one of the developing technologies that offer great promise for the cleanup of soils contaminated with heavy metals. A numerical model was formulated to simulate copper (Cu) transport under an electric field using one-dimensional diffusion-advection equations describing the contaminant transport driven by chemical and electrical gradients in soil during the electro-kinetic remediation as a function of time and space. This model included complex physicochemical factors affecting the transport phenomena, such as soil pH value, aqueous phase reaction, adsorption, and precipitation. One-dimensional finite-difference computer program successfully predicted meaningful values for soil pH profiles and Cu concentration profiles. The model considers that: (1) electrical potential in the soil is constant with the time; (2) the effect of temperature is negligible; and (3) dissolution of soil constituents is negligible. The predicted pH profiles and transport of copper in sandy loam soil during electro-kinetic remediation were found to reasonably agree with the bench-scale electro-kinetic experimental results. The predicted contaminant speciation and distribution (aqueous, adsorbed, and precipitated) allow for an understanding of the transport processes and chemical reactions that control electro-kinetic remediation.

Keywords: Copper removal, Soil pollution, Electro-kinetic, Electro-osmosis, Electro-migration, Soil remediation, Activated carbon Barriers.

نمذجة ومحاكاة معالجة الترب الملوثة بالنحاس بواسطة الجمع بين طريقة الامتزاز والطريقة الكهرو حركية

ا.م.د. أياد عبد الحمزة فيصل

م. أحمد علاء حسين

الخلاصة

تعد الطريقة الكهروحركية من الطرق الحديثة والواعدة القابلة للتطوير لمعالجة الترب الملوثة بالعديد من الملوثات كالمعادن الثقيلة. ان كفاءة الطريقة الكهرو حركية تعتمد على عدة عوامل تم دراسة العديد منها في الدراسة الحالية من خلال اعداد نموذج رياضي لمحاكاة عملية انتقال ايون النحاس (الملوث) عند تسليط تيار كهربائي باستخدام معادلة الانتشار ذات البعد الواحد لمحاكاة انتقال الملوث كهربائياً وكيميائياً في التربة مع الزمن والمسافة خلال تطبيق الطريقة. اشتمل النموذج على عدة عوامل فيزيائية وكيميائية تؤثر في ظاهرة انتقال الملوث كالدالة الحامضية والتفاعلات الكيميائية للطور المائي والامتزاز والترسيب. تم حل النموذج الرياضي بطريقة الفروقات المحددة وقد نجح النموذج بالتنبؤ بقيمة الدالة الحامضية وتركيز الملوث في التربة. تم اعتماد عدد من الفرضيات في النموذج الحالي وهي: (1) الجهد الكهربائي ثابت مع الزمن في التربة. (2) اهمال تأثير درجة الحرارة. (3) اهمال تحلل مكونات التربة. من خلال مطابقة نتيجة التجارب العملية مع نتائج النموذج الرياضي ظهر تطابق معقول ومفسر في تغير الدالة الحامضية وتركيز الملوث مع الزمن والذي وفر فهما حقيقيا لعملية انتقال الملوث تحت تاثير تسليط التيار الكهربائي والتفاعلات الكيميائية عند استخدام الطريقة الكهرو حركية.

الكلمات الرئيسية: معالجة النحاس، تلوث التربة، الطريقة الكهروحركية، معالجة التربة، حواجز مملوءة بالكاربون المنشط

INTRODUCTION

Recently, it has been reported that soil contamination by heavy metals is increasing in various sites including residential areas near industrial complexes and reservoirs of drinking water. This contamination is found in more than 65% of superfund sites in the United States, and in rice paddies in Taiwan and Japan. It has an enormous impact on the quality of ground water, soil and associated ecosystems. However, the solubility and extent of these contaminants in the subsurface system is influenced by the chemistry of the soil and groundwater. Factors such as pH, redox potential (Eh), cation exchange capacity (CEC), and complexation/chelation with organic matter directly affect on the metal solubility (Evanko and Dzombak, 1997; Kim et al., 2003; Saeedi et al., 2009).

One of the emerging technologies to clean up heavy metals contaminated soils is electro-kinetic remediation technique, which has been proven to be a very effective tool to clean up contaminated low hydraulic permeability fine grained soils (Caliman et al, 2011; Virkutyte et al., 2002; Baraud et al, 1997, 1999; Acar, and Alshawabkeh, 1993).

Electro-kinetic remediation, variably named as electro-kinetic soil processing, electro-migration, electrochemical decontamination or electroreclamation, uses electric currents to extract radionuclides, heavy metals, certain organic compounds, or mixed inorganic species and organic wastes from soils and slurries (Acar et al, 1995). The electro-kinetic can be used in combination with other cleanup techniques (Saeedi et al., 2009; Chung Lee, 2007; Greičiūtė and Vasarevičius, 2007). These technologies apply a low current density to contaminated soil in order to mobilize contaminants in the form of charged species. The current is applied by inserting electrodes into the subsurface and relying on the natural conductivity of the soil (due to water and salts) to affect movement of water, ions and particulates through the soil. Water and/or chemical solutions can also be added to enhance the recovery of metals by this process. Positively charged metal ions migrate to the negatively charged electrode (cathode), while metal anions migrate to the positively charged electrode (anode). The metals can be removed by a variety of processes, including electroplating at the electrodes, precipitation / co-precipitation at the electrodes, complexation with ion exchange resins, or by pumping the water from the subsurface and treating it to recover the extracted metals (Evanko and Dzombak, 1997). The electro-kinetic remediation method can be used in-situ or with excavated soil. Metals as soluble ions, bound to soils as oxides, hydroxides and carbonates are removed by this method (Acar et al., 1995).

The low-level direct current results in physico-chemical and hydrological changes in the soil mass, leading to species transport by coupled mechanisms. Electrolysis of water produces hydrogen ions in the anode compartment Eq. (1) and the acid front migrates across the soil cell and makes contaminants desorbed from soil surfaces, resulting in an initiation of electro-migration, i.e. the transport of ions and polar molecules in electric field. Electric potential also leads to electro-osmosis, i.e. the flow of an ionic liquid under the action of an applied electric field relative to a charged surface. Electro-migration and electro-osmosis are the important mechanisms in the electro-kinetic soil processing which remove contaminants from soil (Kim et al., 2001). One of main defects of the conventional electro-kinetics is precipitation of hydroxides near the cathode due to generation of hydroxyl ions by water electrolysis in the cathode compartment Eq. (2), resulting in decrease of the effectiveness of the technology (Kim et al., 2003).

Anode: $2H_2O - 4e^- \rightarrow O_2(g) + 4H^+$ (1)

Cathode: $4H_2O + 4e^- \rightarrow 2H_2(g) + 4OH^-$ (2)

The generated hydrogen and hydroxyl ions are transported through specimen in opposite directions by electrical migration, diffusion and advection. The advance of base front is slower than the advance of the acid front because of the counteracting electro-osmotic flow and also because the ionic mobility of H^+ is about 1.76 times that of OH^-. Consequently, the acid front dominates the chemistry across the specimen except for small sections close to the cathode (Saeedi et al., 2009). In order to be mobile in the electric field, heavy metals must be present in the dissolved phase of the soil. The desorption and mobilization of most heavy metals during the remediation process is catalyzed by an acidic front that develops from the anode end of the soil (Ouhadi et al., 2010).

In this study electro-kinetic remediation technique coupled with activated carbon barrier was investigated to show the ability of activated carbon barrier to prevent the reverse electro-osmotic flow which has adverse effect on the Cu removal and its migration direction, also in this study, a numerical model was developed to understand the mechanics of migration during the electro-kinetic soil remediation and predict electro-kinetic transport in general, and investigate the specific system of the electro-kinetic transport of Cu in soil at laboratory scale. The model results were then compared with the experimental results. In this way, a more enlightened understanding of the results and the adequacy of the theoretical formulation and assumptions employed in the model can be postulated.

THEORY

Application of electric and chemical gradients to soil-water-contaminant system initiates transport of matter and energy with resultant fluxes of fluid and mass through soil media. A set of partial differential equations (PDEs) describing fluxes and conservation of fluid and mass is presented and formulated here. A model was developed to understand the mechanics of migration during the electro-kinetic soil remediation. The model mainly includes the combined effects of electro-migration of a copper species, convection due to electro-osmosis and diffusion. Chemical equilibrium expression, sorption of chemical species and hydrolysis reactions are also considered in the model. For simplicity, the following assumptions are adopted in this theoretical formulation:

1. System is considered as a one dimension.
2. The soil media is isotropic, homogeneous, saturated, and negatively charged.
3. The cell is isothermal.
4. All fluxes are linear functions of potential and hydraulic gradient.
5. Electrophoresis is not considered.
6. Instantaneous equilibrium is assumed locally within the time scale of transport for all chemical reactions.
7. The main species taken into account are $\mathrm{Cu^{2+}}$, $\mathrm{H^{+}}$, and $\mathrm{OH^{-}}$.

Fluid flux due to electrical gradient, i.e. electro-osmotic flow rate (J_w in m s^{-1}), through fine-grained soils can be expressed as:

$$J_w = -k_{eo} \nabla \Phi \tag{3}$$

where k_{eo} (m^2 V^{-1} s^{-1}) is the electro-osmotic permeability coefficient and Φ (V) is the electric potential (Kim et al., 2004).

The value of k_{eo} has been assumed to be constant in numerous electro-kinetic models. Mass flux of chemical species is caused by different mechanisms. Diffusive mass flux is mass transport due to chemical gradient, and electromigrative mass flux is mass transport of charged species under an electric potential gradient. In addition, electro-osmosis causes the advective mass flux due to electrical gradients. Therefore, the total mass flux of chemical species includes diffusive, electromigrative, and advective mass fluxes. The diffusive mass transport of chemical species under chemical gradients in soil media is described by Fick's first law (Kim et al., 2004):

$$J_i^d = D_i^* \nabla (-c_i) \tag{4}$$

where J_i^d (mol m^{-2} s^{-1}) is the diffusive mass flux of the ith chemical species, D_i^* (m^2 s^{-1}) is the effective diffusion coefficient of the ith chemical species, and c_i (mol m^{-3}) is the concentration of the ith chemical species in aqueous phase. The effective diffusion coefficient of the ith chemical species in the porous medium, D_i^*, is expressed by the respective diffusion coefficient in free solution D_i (m^2 s^{-1}).

$$D_i^* = n\, \tau\, D_i \tag{5}$$

where n is the porosity of the soil and τ is the tortuosity factor of the soil medium. Typical values of τ are reported in the range 0.01 to 0.67 (Kim et al., 2003).

The electromigrative mass flux of chemical species under electrical potential gradient is described by:

$$J_i^{em} = u_i^* c_i \nabla (-\Phi_i) \tag{6}$$

where J_i^{em} (mol m^{-2} s^{-1}) is the electromigrative mass flux of the ith chemical species, u_i^* (m^2 V^{-1} s^{-1}) is the effective ionic mobility of the ith chemical species.

The effective ionic mobility, u_i^*, describes the velocity of the ion in soil pores under electric field. Even though the accurate measurement of the value is significantly difficult, the value can be estimated theoretically using the Nernst-Einstein relation between the molecular diffusion coefficient, D_i, and the ionic mobility, u_i (m^2 V^{-1} s^{-1}) (Kim et al., 2004):

$$u_i^* = \frac{D_i^* z_i F}{RT} = n\tau u_i \tag{7}$$

where z_i is the charge of the ith chemical species, F is the Faraday's constant (96,485 C mol^{-1}), R is the universal gas constant (8.3144 J K^{-1} mol^{-1}), T is the absolute temperature (K). The values of ionic mobilities and effective ionic mobilities are negative for anions and positive for cations (Kim et al., 2004; Yu and Neretnieks, 1996; Yu and Neretnieks, 1997).

The advective mass flux of chemical species due to electro-osmotic advection under electrical potential gradient is expressed as:

$$J_i^{eo} = c_i J_w = c_i k_{eo} \nabla(-\Phi) \tag{8}$$

Consequently, the total mass flux will be the summation of Eqs. (4), (6) and (8):

$$J_i = D_i^* \nabla(-c_i) + c_i(u_i^* + k_{eo})\nabla(-\Phi) \tag{9}$$

The PDE describing transient mass transport of species i is expressed using the law of mass conservation (Kim et al., 2004):

$$n\frac{\partial c_i}{\partial t} = -\nabla J_i + nR_i \tag{10}$$

where R_i is the production rate of the ith aqueous chemical species due to chemical reactions. Consequently, the one-dimensional PDEs describing the transport of chemical species can be obtained by combining the equation of total mass flux (Eq. 9) and the equation of mass conservation (Eq. 10) as follows:

$$n\frac{\partial c_i}{\partial t} = D_i^* \frac{\partial^2 c_i}{\partial x^2} + (u_i^* + k_{eo})\frac{\partial c_i}{\partial x}\frac{\partial \Phi}{\partial x} + c_i(u_i^* + k_{eo})\frac{\partial^2 \Phi}{\partial x^2} + nR_i \tag{11}$$

CHEMICAL REACTIONS

Eq. 11 may be simplified by expanding the production term, R_i, to account chemical reaction such as aqueous phase, adsorption, and precipitation / dissolution reactions as follow:

$$R_i = R_i^{aq} + R_i^{ad} + R_i^{P} \tag{12}$$

where R_i^{aq} is the production rate of the ith aqueous chemical species due to aqueous phase reaction, R_i^{ad} is the production rate of the ith aqueous chemical species due to adsorption reaction, and R_i^{P} is the production rate of the ith aqueous chemical species due to precipitation reaction. The chemical reactions are generally described by equilibrium (instantaneous equilibrium), as previously mentioned in assumptions. For the aqueous phase reaction, the following water-autoionization reaction is taken into account in this study (Kim et al., 2003):

$$H_2O \rightleftharpoons H^+ + OH^- \tag{13a}$$

$$\Delta c_H = \Delta c_{OH} \tag{13b}$$

$$R_H^{aq} = R_{OH}^{aq} \tag{13c}$$

$$c_H c_{OH} = K_w = 10^{-14} \tag{13d}$$

For investigation of adsorption of species on the soil particles, the following relation has been generally used (Kim et al., 2003):

$$R_i^{ad} = -\frac{\rho}{n}\frac{\partial c_i^{ad}}{\partial t} = -\frac{\rho}{n}\frac{\partial c_i^{ad}}{\partial c_i}\frac{\partial c_i}{\partial t} \tag{14}$$

where ρ is the bulk dry density of the soil, and c_i^{ad} is the adsorbed concentration of the ith species per unit mass of the soil solids. The equilibrium partitioning between the adsorbed phase and the aqueous phase of the chemical species are generally measured under constant temperature and applied pressure, and the adsorption isotherms, i.e., the relation between aqueous concentration, c_i (mol m^{-3}), and adsorbed concentration, c_i^{ad} (mol kg^{-1}), are determined. Based on the assumption of the instantaneous equilibrium and linear adsorption reaction, the distribution of adsorbed concentrations can be related to the change of aqueous concentrations:

$$\frac{\partial c_i^{ad}}{\partial c_i} = K_i^d \tag{15}$$

where K_i^d (m^3 kg^{-1}) is called the distribution coefficient of the ith species. A retardation factor of the ith species, R_i^d, has been introduced and used in modeling transport of species in porous media, based on linear adsorption isotherm (Kim et al., 2003):

$$R_i^d = 1 + \frac{\rho K_i^d}{n} \tag{16}$$

The retardation factor of the *i*th species (R_i^d) indicates the relative rate of transport of a nonsorbed species to that of a sorbed species. Since $R_i^d > 1.0$, the transport time for sorbed species greater than the transport time for nonsorbed species.

During the electro-kinetic soil remediation, heavy metal contaminants in soils precipitate near the cathode region due to high pH caused by transport of hydroxide ions from the cathode compartment. For this reason, the precipitation reaction must be taken in the theoretical formulation for transport of species in soils. In this study, the target metal contaminant is Cu^{2+}, and its precipitation reaction is taken into account using solubility product:

$$Cu(OH)_2 \rightleftharpoons Cu^{2+} + 2OH^- \quad (17a)$$

$$c_{OH}^2\, c_{Cu} \le K_{sp}^{Cu(OH)_2} = 3.09 \times 10^{-20} \quad (17b)$$

where $K_{sp}^{Cu(OH)_2}$ is the solubility product of the reaction. Combining the water-autoionization reaction and precipitation reaction, the total change of OH^- concentration due to both reactions was obtained as follows:

$$\Delta\, c_{OH} = \Delta\, c_H + 2\Delta\, c_{Cu} \quad (18a)$$

$$R_{OH} = R_H^{aq} + 2R_{Cu}^{P} \quad (18b)$$

Eq. (17a) show that the dissolution of 1 mole of copper hydroxide will generate 1 mole of Cu^{2+} and 2 moles of OH^-. This means that the change in OH^- molar concentration duo to copper hydroxide dissolution/precipitation reaction is twice the change of Cu^{2+} molar concentration. In the same time, the change in molar concentration of OH^- due to water auto ionization equals the change in molar concentration of H^+. Consequently, Eq. (18 a) expresses the total change in OH^- concentration due to both reactions described above (Acar and Alshawabkeh, 1997).

The PDEs expressing H^+, OH^- and Cu^{2+} transport under chemical and electrical gradients are described by the following equations:

$$n\, R_H^d \frac{\partial c_H}{\partial t} = D_H^* \frac{\partial^2 c_H}{\partial\, x^2} + (u_H^* + k_{eo}) \frac{\partial c_H}{\partial x} \frac{\partial \Phi}{\partial x} - n\, R_H^{aq} \quad (19)$$

$$n \frac{\partial c_{OH}}{\partial t} = D_{OH}^* \frac{\partial^2 c_{OH}}{\partial\, x^2} + (u_{OH}^* + k_{eo}) \frac{\partial c_{OH}}{\partial x} \frac{\partial \Phi}{\partial x} - R_{OH}^{aq} \quad (20)$$

$$n \frac{\partial c_{Cu}}{\partial t} = D_{Cu}^* \frac{\partial^2 c_{Cu}}{\partial\, x^2} + (u_{Cu}^* + k_{eo}) \frac{\partial c_{Cu}}{\partial x} \frac{\partial \Phi}{\partial x} - R_{Cu}^{ad} - R_{Cu}^{P} \quad (21)$$

where R_H^d is the retardation factor of H^+.

In order to explain the movement of species (Cu^{2+}, H^+, OH^-) 3 partial differential equations are used. In addition 4 algebraic equations are used to describe the chemical reaction of Cu^{2+} in the pore fluid (Eqs. 13d, 17b, 18b) and adsorption isotherm of Cu^{2+}.

To obtain a numerical solution, the 3 initial conditions and 6 boundary conditions was applied. For every partial difference equation, 1 initial condition and 2 boundary conditions are required in one dimension. Table 1 summaries the initial and boundary conditions applied in the MATLAB program prepared here to solve the electro-kinetic problem. For H^+ and OH^- ions, the boundary conditions for Case I was assumed to be exponentially changing as a function of time (Fig.1). This assumption was based on the measured pH in the electrode compartments of the electro-kinetic experiments.

An explicit method among finite difference methods was applied to the PDE describing the transport of fluid and contaminant through soil under electrical field. Eq. (19) is formulated according to the following: for time, forward difference was used; for space, backward difference was used for simple partial difference; and center difference was used for quadratic partial difference:

$$C_{H_i}^{n+1} = C_{H_i}^{n} + \left(\frac{\Delta t}{n\, R_H^d}\right)(D_H^*)\left(\frac{C_{H_{i+1}}^n - 2C_{H_i}^n + C_{H_{i-1}}^n}{\Delta\, x^2}\right) + \left(\frac{\Delta t}{n\, R_H^d}\right)(u_H^* + k_{eo})\left(\frac{\partial \Phi}{\partial x}\right)\left(\frac{C_{H_i}^n - C_{H_{i-1}}^n}{\Delta x}\right) - nR_H^{aq} \quad (22)$$

where the superscript $n+1$ and n are the next and present time step, respectively; $\Delta t = t^{n+1} - t^n$ is the time step size, and $i, i+1, i-1$ are the grid identification (Fig.2).

Similar to the H^+ equation, the migration of OH^- Eq. (20) and Cu^{2+} Eq. (21) can be formulated in the same procedure. The formulation of discretized algebraic equations was followed by development of computer program, which was written in MATLAB R2009b. The flowchart shows the analysis process flow of this program is presented in Fig.3.

EXPERIMENTAL METHODOLOGY

1. Electro-kinetic Test Setup

Fig.4 shows the schematic of the electro-kinetic test setup used for this study. The setup consists of an electro-kinetic cell, two electrode compartments, a power supply, and a multi-meter. The glass electro-kinetic cell (Fig.22) has an inside dimensions 40 cm long 6 cm width, and 10 cm high. The actual length of the soil specimen inside this cell equal to 18 cm. Activated carbon was used as a barrier in the electro-kinetic cell between the soil sample and cathode compartment with length of 5 cm. Each electrode compartment consists of a valve to control the flow in the cell, a slotted graphite electrode and filter paper. Perforated plastic plates were used to separate the activated carbon barrier from soil at one end and from cathode electrode from the other end. Anode electrode was a perforated graphite plate with dimensions of 10 x 6 x 0.3 cm. While, the cathode was graphite rode of 5 cm diameter. A power source (LODESTAR LP3005D) was used to apply a constant voltage to the electrodes, and a multi-meter was used to monitor the voltage and measure the current flow through the soil sample during the test.

2. MATERIALS

After considering various heavy metals, copper was chosen as the contaminant fluid. It was added in the form of copper chloride dihydrate with a formula of $CuCl_2.2H_2O$ from AVONCHEM Company (UK). $CuCl_2.2H_2O$ has a molecular weight of 170.48 g/mole and atomic weight of copper ions is 63.546 g/mole. To prepare a soil sample with copper concentration equal to 750 mg/kg and initial moisture content equal to 35% by weight, 2.88 g of $CuCl_2.2H_2O$ dissolves in 500 ml of distilled water and 350 ml of this solution is added to 1 kg of dry soil.

Table 2 summarizes the composition and properties of the soil. The soil was clean and well-sorted which needed to an additional sieving to achieve satisfactory uniformity.

Granulated activated carbon (GAC) was used in the present electro-kinetic cell. It was sieved into (30/35) mesh with geometric mean diameter of (0.55 mm). The Activated carbon was washed three times in distilled water and dried at 105 °C for 24 hours before it was used.

3. EXPERIMENTAL DESIGN

Two different tests were performed to investigate the effect of the electro-kinetic remedial efficiency in the type of local natural soil. Table 3 illustrates the test conditions.

For the first test (EK-1), tap water (EC=251 µS/cm, pH=7.2) was used in both the anode, mid, and cathode compartments. For the second test (EK-2), purging solution was a tap water associated with adjustment of pH in the anode, mid, and cathode compartments to maintain the pH range of (6.6-7.1). This was achieved by adding nitric acid (HNO_3) at the cathode and mid compartments. Whereas, sodium hydroxide (NaOH) was added at anode compartment. These tests gave the variation of pH front propagation, metal concentrations, electrical conductivity as well as the electrical current and electro-osmotic flow values with the time.

4. TESTING PROCEDURE

The soil samples were artificially contaminated with copper ions in the electro-kinetic tests. The required amount of the dihydrate copper chloride that would yield the desired concentration was weighed and then dissolved individually in distilled water. The contaminant solution was then added to 1kg of the dry soil and mixed thoroughly with a plastic spatula in polyethylene container. A total of 350 ml of distilled water (35% moisture content) was used to represent typical field moisture conditions. The contaminated soil was then placed in the electro-kinetic cell in layers and compacted uniformly using wooden rod. The exact weight of the soil used in the cell was determined and the soil was equilibrated for 24 hrs. The filter papers were inserted at the ends of the soil sample and the activated carbon barrier.

The electrode and mid compartments in (EK1 & EK2) were filled with potable water. Potable water was selected because it is the most likely source of replenishing fluid at most field contaminated sites. The elevation of water level in the electrode compartment was kept constant to prevent a hydraulic gradient from forming across the specimen. The electro-kinetic cell was then connected to the power supply and a constant DC voltage gradient was applied to the system. The electric current across the soil sample as well as the water flow, pH, and electrical conductivity in both the anode, cathode, and mid compartments as well as injection wells were measured at different time periods throughout the duration of the experiment. The test was terminated when the current stabilized, when no significant change in the water flow was observed.

At the end of each test, the soil specimen and activated carbon were extruded from the cell. The soil specimen was sectioned into five parts and each part was weighed and subsequently preserved in a glass container. From each soil section, 5 g of dry soil was taken and mixed with 12.5 ml distilled water. The mixture was shaken thoroughly by hand for several minutes and the solids were then allowed to settle for 1 h. pH and electrical conductivity of the soil was measured (Hansen et al., 2007).

5. CHEMICAL ANALYSIS

Copper in different soil sections were extracted by performed acid digestion in accordance with the Danish Standard DS 259:2003 (30 min at 200 kPa (120 °C)) by adding 20 ml 1:1 HNO_3 to 1g dry matter and treating the sample in autoclave. The liquid was separated from the solid particles by vacuum through a 0.45 µm filter and it is diluted to 100 ml. The copper concentration was determined by atomic absorption spectrophotometer (AAS) (novAA 300) (Hansen et al., 2007).

Precautions were taken in order to ensure the accuracy of the test results. These precautions included: (1) new electrodes and filter papers were used for each experiment; (2) the electro-kinetic cell and compartments were soaked in a dilute acid solution for 24 hour and then rinsed first with tap water and finally with distilled water to avoid cross contamination between the experiments; and (3) checking the atomic absorption calibration after testing every five samples. Copper concentrations in the soil samples are measured at Laboratory of Ministry of the Environment. While, soil analyses are carried out at State Company of Geological Survey and Mining, Ministry of Industry and Minerals.

RESULTS AND DISCUSSION

1. Experiment one (EK-1)

The experiment (EK-1) was conducted as a baseline for other experiments, it was run with tap water as purge solution without adjusting pH at anode, mid, and cathode compartment to show the behavior of unenhanced (conventional) electro-kinetic remediation. The duration of (EK-1) was seven day. Fig.5 show the variation of pH of the fluid at anode (anolyte), Mid, and cathode (catholyte) recorded during the experiment. The tap water initially introduced into the anode, mid and cathode reservoirs had a pH value around 7.2. Due to the applied electric potential, the electrolysis of water produced H^+ at the anode and OH^- at the cathode. As a result, pH of anolyte (anode solution) decreased, while the pH of mid and catholyte (cathode solution) increased.

Compared to the initial pH values, pH changed significantly in the anode and cathode compartments in the test. The results show that considerable electrolysis reactions occurred at electrodes in the test, and the measured pH values are consistent with the values reported in the literature (Acar and Alshawabkeh, 1993). Due to high pH at mid and cathode compartment the ionic species precipitated as hydroxides forms and limit the remediation efficiency. For this reason the mid and cathode compartment should be lowered pH to avoid the generation of hydroxide and its transport into the soil.

The initial electrical conductivity (EC) value of the tap water used in both the anode and cathode reservoirs equal to 251µS/cm (Fig.6). The EC values of anolyte and mid increased and finally decreases. However, the EC values of catholyte increased to 1.74 mS/cm. duo to migrating of negative ionic species to the cathode. Relatively high EC values at the catholyte indicated higher ionic concentration in cathode electrode solution.

Fig.7 shows the profile of electric current during the tests the current initially was decreased in 0-7 hour and increases to 16.8 mA after 36 hour current decreased and finally stabilized to 3.7-3.8 mA.

Direction of fluid flow was from the anode to the cathode reservoirs (zeta potential $\zeta < 0$). Fig.8 shows the plot for cumulative volume of effluent versus time. The effluent flow increased with time and finally stopped because clogging of pores that happen from deposition in the soil of compounds such as metal hydroxides which may be formed by reaction between hydroxyl ions near the cathode and heavy metal contaminants and eventual cessation of flow (Page and Page, 2002).

Furthermore, the calcium precipitation close to the cathode clogged the soil pores; restraining further transport of heavy metal ions for removal (Ouhadi et al. 2010).

Fig.9a shows the Cu concentration vs. normal distance from the anode with respect to starting values in the soil (750 mg kg). As shown, the Cu migrated from the anode and accumulated in the sections near the mid compartment (toward the cathode). Fig.9b,c shows the pH and EC changes vs. normal distance from the anode of the treated soil. The generated hydrogen and hydroxyl ions are transported through specimen in opposite directions by electrical migration, diffusion and advection. The advance of base front is slower than the advance of the acid front because of the counteracting electro-osmotic flow and also because the ionic mobility of H^+ is about 1.76 times that of OH^- (Saeedi et al. 2009). Where the acid and base fronts meet, water is formed resulting in a sharp change in pH, which affects the solubility of contaminants and their adsorption to the soil and. An added complication is the effect of pH on the soil minerals. Soil constituents, including clay minerals, may dissolve because of the changing composition of the pore solution. An increase in the concentrations of certain ions of, e.g., Mg, Al, and Fe is often seen as a result of increased acidity and others of, e.g., Si and Al with increased alkalinity. Al ions are commonly detected in pore solutions of soils which have undergone electro remediation. Changes in the pH profiles in the soil had a great influence on contaminant migration; tests conducted in the present study showed that pH has a significant impact on Cu migration in the soil. Due to the low pH at the anode, the Cu concentration decreased. The high pH indicated that some OH^- ions were reaching the soil and possibly interfering with the mobility of copper ions. The high pH environment was favorable to make $Cu(OH)_2$ which precipitate near the cathode sections and decrease the soil conductivity. According to this fact, the higher Cu concentrations were found near the cathode sections (Page and Page, 2002).

A certain amount was found in the anode compartment. It was also suggested that copper found in the anode compartment may be due to its capability of forming complexes with different legends present in soils (Ahmed, 2004; Virkutyte et al., 2002).

The drawbacks of electro-kinetic process were the amount of (calcite or carbonate) ($CaCO_3$). The presence of carbonate in soils causes an increase in buffering capacity; the alkaline pH of soil rich in carbonate does not significantly vary in electro-kinetic contaminant remediation. Consequently, heavy metal contamination is retained in precipitated hydroxide/carbonate forms. As a result, the efficiency of electro-kinetic remediation decreases (Ouhadi et al. 2010).

According to the present experimental work, activated carbon prevents the reverse electro-osmotic flow which has negative effect on direction and magnitude of Cu migration during electro-kinetic process. Due to high sorption capacity of activated carbon, small amount of Cu^{2+} ions was absorbed by activated carbon due to competitive of the ions of salts available in the soil samples with Cu^{2+} ions (Saeedi et al., 2009).

2. Experiment two (EK-2)

The experiment (EK-2) was conducted at the same condition of experiment (EK-1) with adjusting pH at anode, mid, and cathode at (6.6-7) during the process by adding NaOH to anode and HNO_3 to mid and cathode. The duration of (EK-2) was four day. Fig.10 shows EC measured during the (EK-2). pH was adjust to prevent precipitation of ionic species as hydroxides forms and to avoid the generation of hydroxide at cathode compartment and its transport into the soil and limit the remediation efficiency of process. Adjust pH caused increase in EC at anode, mid, and cathode compartments (Fig.10). The current (Fig.11), cumulative volume of effluent versus time (Fig.12), and Removal efficiency was also increased. In soil pH decreased compared to EK-1 (Fig.13b). Soil conductivity increased compared to EK-1 (Fig.13c) as a result to increase EC in anode, mid, and cathode. Fig.13a indicate removal of copper from the soil system in all sections are below the initial concentration profile. Increased copper concentrations were observed near the cathode.

3. Copper Sorption

The EPA batch-type test procedure was adopted here to determine the adsorption of copper on sandy loam soil. Batch adsorption tests for this soil were conducted for seven different soil to solution ratios [1:4, 1:10, 1:40, 1:60, 1:100, 1:200 and 1:500 (mass/volume)] with a constant solution volume of (50 ml) and Cu concentration of 1000 mg/l. The amount of solute remaining in solution after 24 h is plotted against the soil: solution ratio as shown in Fig.14. The bounded area approximates the desired solute concentration after 24 h of mixing based on 10% to 30% solute adsorption (USEPA, 1992). A ratio of soil: solution 1: 120 with equilibrium time of 24 h was chosen to study copper adsorption by the sandy loam sample. Batch adsorption tests were conducted with three different initial concentrations (100, 500, and 1000 mg/l) at four different constant pH conditions (1, 3, 5, and 7) (Fig.15& 16). The pH of the samples was adjusted by using 0.1M HNO_3 or 0.1M NaOH. Samples were shaken at room temperature (25 °C) with 180 rpm for 24 hour then filtered using Wattman filter paper. The supernatant was analyzed using an atomic absorption spectrophotometer (AAS) to determine the concentration of total copper.

4. MODEL VERIFICATION

4.1 Model Predictions

Parameters and constants related to the sandy loam soil adopted here for verification were evaluated, either through laboratory tests or through approximation using literature data (Table 4). Porosity, bulk density and electro-osmotic permeability coefficient (k_{eo}) of this soil were experimentally determined. The tortuosity factor (τ) for sandy loam soil modeled was not determined experimentally, but a value of 0.25 was used in this study. Typical values of τ vary in the range 0.01–0.67 according to the soil type, and vary over a narrow range between 0.25 and 0.35 for sandy loam soil (Acar and Alshawabkeh, 1997). The effective diffusion coefficients and effective ionic mobilities of species are presented in Table 5., which were calculated by the diffusion coefficients and ionic mobilities at infinite dilution. The algebraic equation describing the adsorption of Cu^{2+} onto sandy loam soil was developed based on the linear and pH-dependent adsorption isotherm determined experimentally as described in (Sec.8.3). This relation was used for the calculation of adsorbed concentrations of copper species in the model.

Soil pH values across the electrodes change from as low as 2 to as high as 12 with time in the first simulation (case1 corresponding to EK-1), (Fig.17a) whereas pH values of the second simulation (case 2 corresponding to EK-2) were maintained on the values of 7 at each the anode and cathode compartments (Fig.17b). The pH jump point for EK-1 after a 7-day run is observed in the region near the middle of the soil bed (normalized distance from anode is about 0.55),and it migrates toward the cathode side with time, as shown in Fig.17a. It is caused by the consumption of hydroxyl ions migrating from the cathode compartment as a result of the water production with hydrogen ions and the precipitation reaction with aqueous phase Cu^{2+} species. While the pH across the soil bed in the EK-2 approaches the value of pH in the electrodes compartments as shown in Fig.17b.

The concentration profiles of different forms of Cu^{2+} for first simulation are shown in Fig.18. The initial total concentration of Cu^{2+}in both tests (EK-1 and EK-2) are equal to (750 mg/kg), and all the Cu^{2+} species initially exist as adsorbed form. Accordingly, the initial concentration of the aqueous phase species is zero across the soil bed. This adsorbed species can be transported only if the species are released in the pore fluid with the decrease of soil pH. This means that the transport occurs only when Cu^{2+} exists in the aqueous form, whereas the adsorbed and precipitated forms of this metal remain immobilized in the soil. According to the linear and pH-dependent adsorption isotherm of Cu^{2+} shown in Fig.17, all the adsorbed Cu^{2+} species can be desorbed and converted into aqueous phase species if the soil pH decreases below about 1. However, the soil pH does not decrease so much (Fig.17), and all the adsorbed species cannot be converted into the aqueous species within most of the soil bed (Fig.18b). As the soil pH decreases down to around 2 for first simulation, the maximum concentration of the aqueous species cannot exceed around 85% of the total concentration (~28.5mol/m^3) as calculated from the linear adsorption isotherm (Fig.17). In contrast the soil pH maintains to around 7 for second simulation. This means that the maximum concentration of the aqueous species cannot exceed around 10% of the total concentration (~3.37mol/m^3). However, the total Cu^{2+}concentration distribution for second simulation is shown in Fig.19.

4.2 Comparison of Model Predictions and Experimental Results

Comparisons between the predicted and experimental pH profiles for tests (EK-1 and EK-2) after specified period of electro-kinetic treatment are depicted in Fig.20. A reasonable agreement between the predicted and the experimental results is observed in Fig.20b. Although there is a significant difference between these results in the Fig.20a, an acceptable trend can be recognized. Due to the formation of H^+ and OH^- ions at the anode and the cathode, respectively, an acid front is generated at the anode whereas a base front is generated at the cathode. As H^+ is cationic in nature, it tends to move toward the cathode. On the other hand, the OH^- is anionic and it tends to move toward the anode. The predicted pH profiles across the sandy loam soil specimen show that the rate of advance of the acid front toward the cathode is faster than that of the rate of advance of the base front toward the anode (i.e., ionic mobility of H^+ is greater than that of OH^-). The predicted pH profiles also show that the acid front meets the base front within 1 to 7 days at a normalized distance approximately equal to 55% of the soil length from the anode. Consequently, the acid front drives the base front back toward the cathode. The simulation results showed that a sharp gradient in the pH was generated at the location where the acid and base fronts meet.

Fig.21 presents a comparison between the model predictions and the experimental results for copper during electro-kinetic remediation. The model predictions show that this metal migrates from the anode toward the cathode in wave fronts during electro-kinetic remediation. A reasonable agreement between the predicted and the experimental results is observed.

However, any variation between the model predictions and experimental results could be attributed to the simplifications and assumptions made in the developed model such as: (1) assuming that the electrical field gradient is constant with time across the soil; (2) neglecting the effect of temperature on the position of the equilibrium; (3) neglecting the salts (such as calcite or carbonate…etc.) adsorption and their adsorption competition with the copper over the solid surface; and (5) neglecting the dissolution reaction of sandy loam soil and its electro-kinetic implications.

CONCLUSIONS

Based on the results obtained from the present numerical model and experimental measurements, the following conclusions can be drawn:

(1) The electro-kinetic removal of copper from low buffering soil (i.e., sandy loam soil, EK-1) using tap water as the purging solution was very low. This removal based on residual soil concentrations was 19.7%. The low removal was attributed to Cu adsorption/precipitation in the cathode region due to high pH. In this test, the pH values at the anode and the cathode were 2 and 12, respectively, indicating that electrolysis reactions were occurred. According to the experimental results of this test, the pH distribution within this soil varied from approximately 6.7 near the anode to approximately 11.4 near the cathode. This pH variation indicates that alkaline conditions existed in the soil during the entire remediation period. The alkaline environment is a result of approximately many salts which were present in the soil and which increased the buffering capacity of the soil. While in EK-2 when pH was adjusted the removal based on residual soil concentrations was 39.12%.

(3) The result show that the coupled technology of electro-kinetic process with activated carbon barrier to remove Cu from sandy loam soil could effectively prevent the reverse electro-osmotic flow which has adverse effect on the Cu removal from soil also the contaminant migration towards the cathode during the tests.

(4) Contaminant migration/removal depends on various factors such as soil pH, remediation time, and sorption/desorption, ionic mobility of contaminant.

(5) Additionally to the experimental part of the study, a model was developed to understand the mechanics of migration. Numerical modeling and experimental study were conducted to simulate Cu transport in sandy loam soil under electrical fields. The model simulations of two cases display good predictions of changes in soil pH and the concentration distributions of Cu species across the soil bed.

REFERENCES

Acar, Y.B., Alshawabkeh, A.N., 1993. Principles of electro-kinetic remediation. Environ. Sci. Technol., 27, 2638-2647.

Acar, Y.B., Gale, R.J., Alshawabkeh, A.N., Marks, R.E., Puppala, S., Bricka, M., Parker, R., 1995. Electro-kinetic remediation: basics and technology status. Journal of Hazardous Materials, 40, 117- I37.

Acar, Y.B., Alshawabkeh, A.N., Parker, R.A., 1997. Theoretical and experimental modeling of multi-species transport in Soils under electric fields. USEPA/600/R-97/045.

Ahmed, H., 2004. Evaluation and enhancement of electro-kinetic technology for remediation of chromium copper arsenic from clayey soil. PHD

Thesis, Florida state University, college of engineering.

Baraud, F., Tellier, S., Astruc, M., 1997. Ion velocity in soil solution during electro-kinetic remediation. Journal of Hazardous Materials, 56, 315-332.

Baraud, F., Tellier, S., Astruc, M., 1999. Temperature effect on ionic transport during soil electro-kinetic treatment at constant pH. Journal of Hazardous Materials, B: 64, 263–281.

Caliman, F.A., Robu, B.M., Smaranda, C., Pavel, V.L., Gavrilescu, M., 2011. Soil and groundwater cleanup: benefits and limits of emerging technologies. Clean Techn. Environ. Policy, 13, 241–268.

Chung, H. and Lee, M., 2007. A new method for remedial treatment of contaminated clayey soils by electro-kinetic coupled with permeable reactive barriers. Electrochim. Acta., 52, 3427-3431.

Evanko, C.R., Dzombak, D.A., 1997. Remediation of metals-contaminated soils and groundwater. Technology evaluation report, TE-97-01. Gound-Water Remediation Technologies Analysis Center, Pittsburgh University, EPA.

Greičiūtė, K., and Vasarevičius, S., 2007. Decontamination of heavy-metal polluted soil by electro-kinetic remediation. GEOLOGIJA, 57, 55-62.

Hansen, H.K., Rojo, A., Ottosen, L.M., 2007. Electro-kinetic remediation of copper mine tailings implementing bipolar electrodes. Electrochimica. Acta., 52, 3355-3359.

Kim, S.O., Moon, S.H., Kim, K.W., 2001. Removal of heavy metals from soils using enhanced electro-kinetic soil processing. Water, Air, and Soil Pollution, 125, 259-272.

Kim, S.O., Kim, J.J. Yun, S.T., Kim, K.W., 2003. Numerical and experimental studies on cadmium (II) transport in kaolinite clay under electrical fields, Water, Air, and Soil Pollution, 150, 135-162.

Kim, S.O., Kim, J.J., Kim, K.W., Yun, S.T., 2004. Models and experiments on electro-kinetic removal of Pb (II) from kaolinite clay. SEPARATION Science and Technology, 39, 1927-1951.

Ouhadi, V.R., Yong, R.N., Shariatmadari, N., Saeidijam, S., Goodarzi, A.R., Safari-Zanjani, M., 2010. Impact of carbonate on the efficiency of heavy metal removal from kaolinite soil by the electro-kinetic soil remediation method. Journal of Hazardous Materials, 173, 87-94.

Page, M.M., Page, C.L., 2002. Electroremediation of Contaminated Soils. Journal of Environmental Engineering (ASCE), 128, 208-219.

Saeedi, M., Jamshidi, A., Shariatmadri, N., Falamaki, A., 2009 . An investigation on the efficiency of electro-kinetic coupled with carbon active barrier to remediate nickel contaminated clay. Int. J. Environ. Res., 3(4), 629-636.

United States Environmental Protection Agency, Batch-Type procedures for estimating soil adsorption of chemicals, EPA/530/SW-87/006-F, April, 1992.

Virkutyte J., Sillanpaa M., Latostenmaa P., 2002. Electro-kinetic soil remediation - critical overview, The Science of the Total Environment, 289, 97-121.

Yu, J.W., Neretnieks, I., 1996. Modeling of transport and reaction processes in a porous medium in an electrical field. Chemical Engineering Science, 51(19), 4355-4368.

Yu, J.W., Neretnieks, I., 1997. Theoretical evaluation of a technique for electro-kinetic decontamination of soils. Journal of Contaminant Hydrology, 26, 291-299.

Table 1: Initial and boundary conditions.

Variables	Initial conditions	Boundary conditions	
		Anode ($x = 0$)	Cathode ($x = L$)
c_{Cu}	$c_{initial}$	Case I: $J_{Cu} = 0.0$ Case II: $J_{Cu} = 0.0$	$J_{Cu} = c_{Cu} J_w$
c_H	$c_{initial}$	Case I: $10^{-(-0.397\ ln\ (t)+3.964)^*}$ Case II: $1\ x 10^{-7}$	$c_H = \frac{10^{-14}}{c_{OH}}$
c_{OH}	$c_{initial}$	Case I: $10^{-(0.406\ ln\ (t)+10.06)}$ Case II: $1\ x\ 10^{-7}$	$c_H = \frac{10^{-14}}{c_{OH}}$

* The time is in hours.

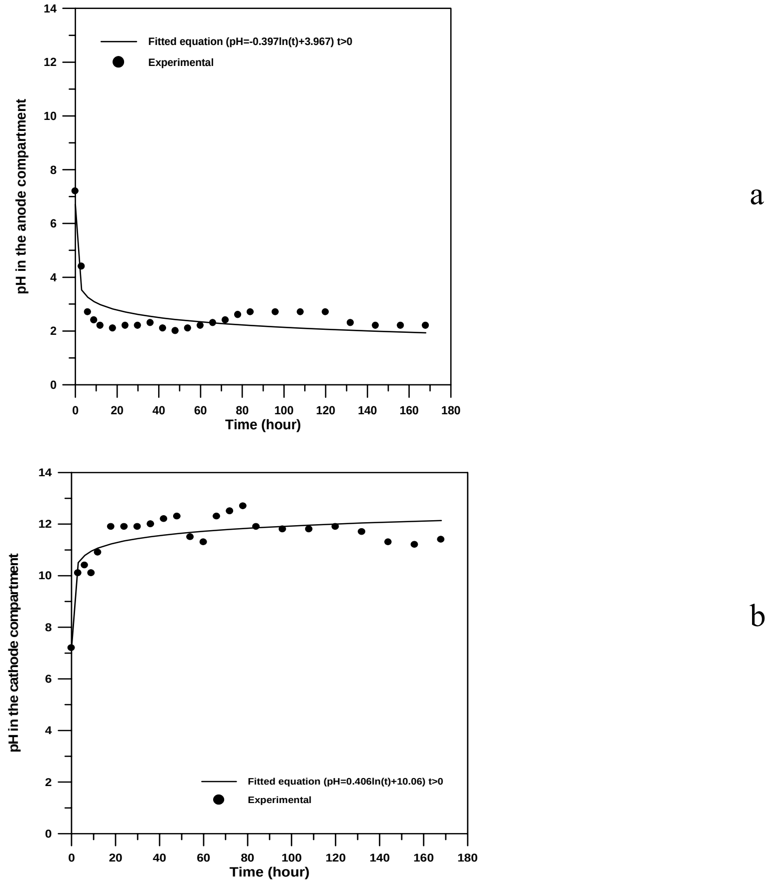

Fig.1: Experimental and theoretical profile of pH: (a) anode compartment and (b) cathode compartment.

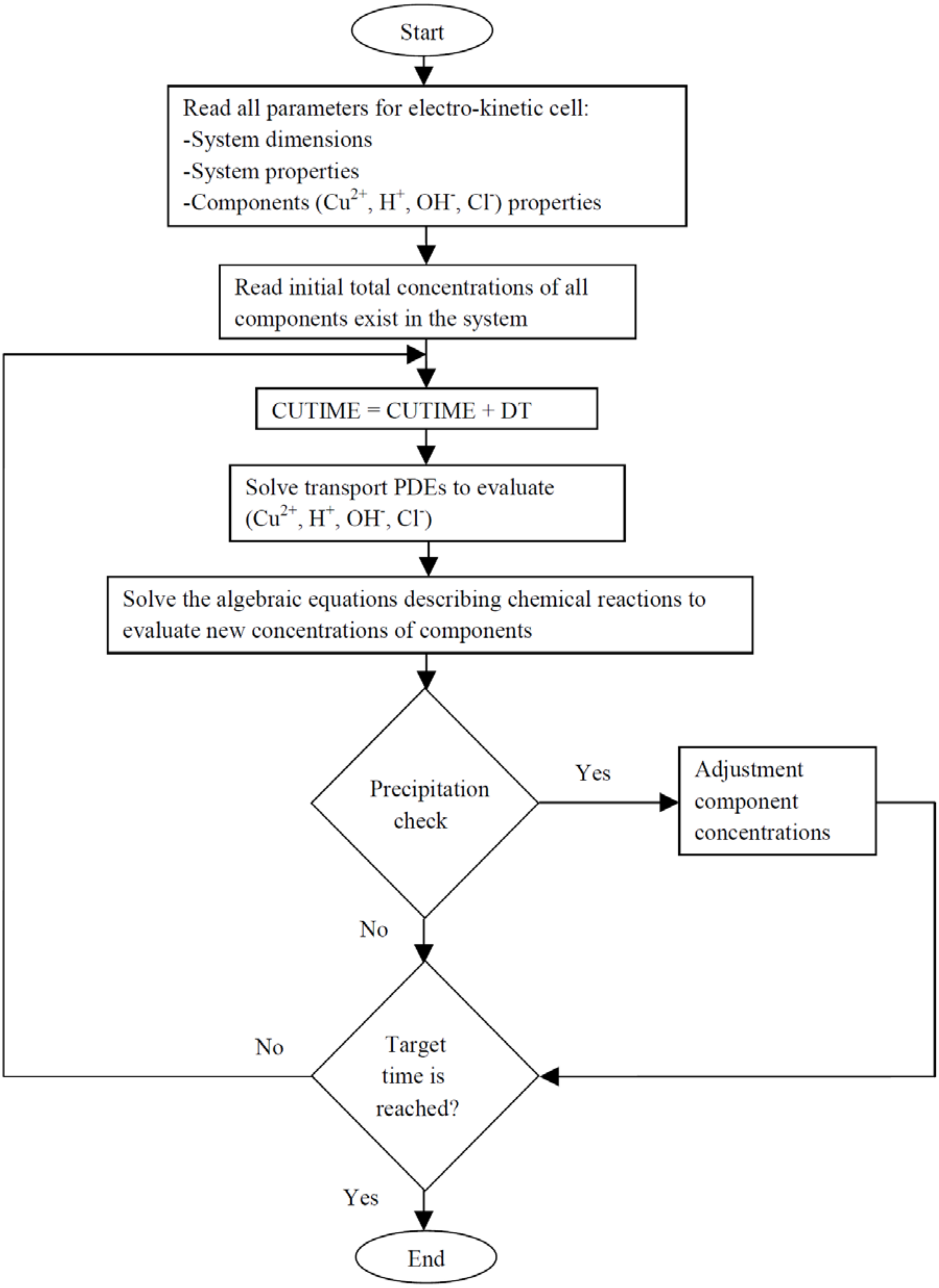

Fig.3: General flow chart for main program.

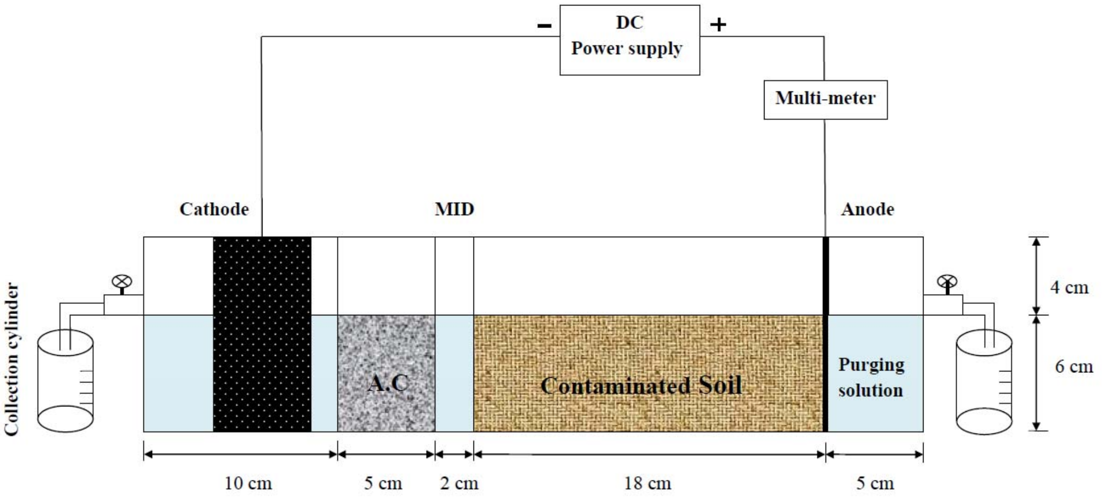

Fig.4: Schematic representation of electro-kinetic cell.

Table 2: Composition and properties of the soil samples.

Property	Sandy loam
Particle size distribution (ASTM D 422) Sand (%) Silt (%) Clay (%)	56 31 13
Atterberg limits (ASTM D 4318) Liquid limit (%) Plastic limit (%) Plasticity index (%)	ND ND ND
Hydraulic conductivity (or coefficient of permeability) (cm s^{-1})	2.7 x 10^{-4}
Cation exchange capacity (meq /100 g)	6.25
pH	7.5
Organic content (%)	0.03
Electrical conductivity EC (µS/cm)	1356
Porosity (n)	0.41

ND: Not detected

Table 3: Electro-kinetic remediation experiments.

Test NO.	Initial water content%	Processing duration (days)	Applied voltage (V)	Purging solution	Purpose Of Exp.
EK-1	35%	7	20	Tap water	Baseline Exp.
EK-2	35%	4	20	Tap water pH(6.6-7.1)	Effect of pH

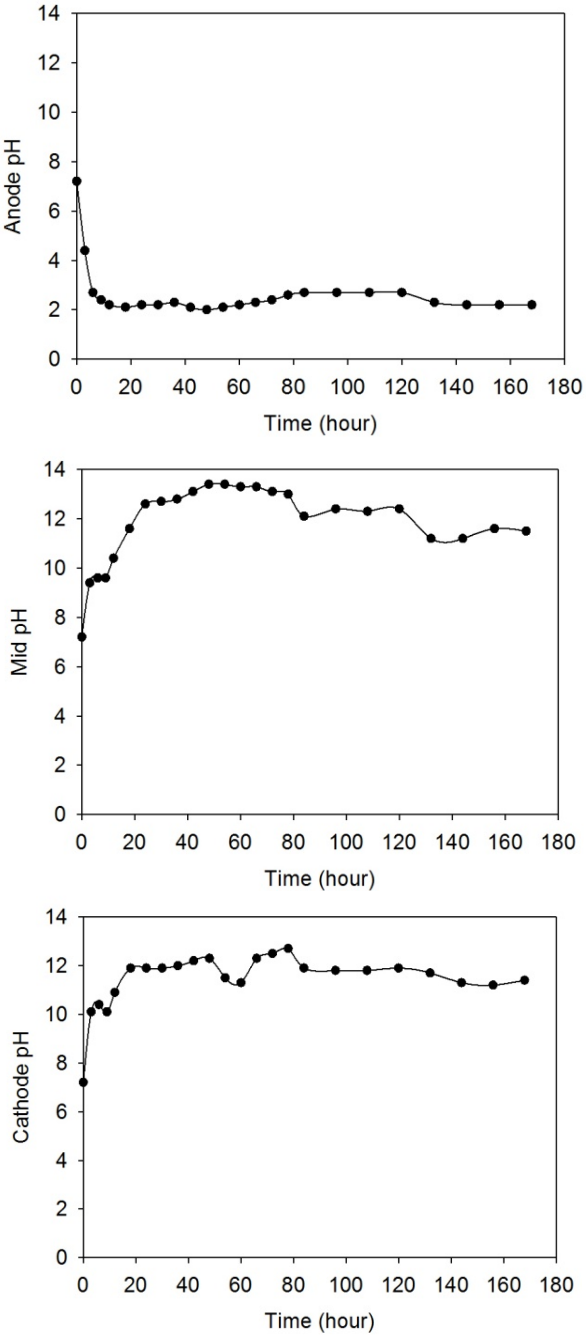

Fig. 5: pH variation in the anode, mid, and cathode compartments versus the time during (EK-1).

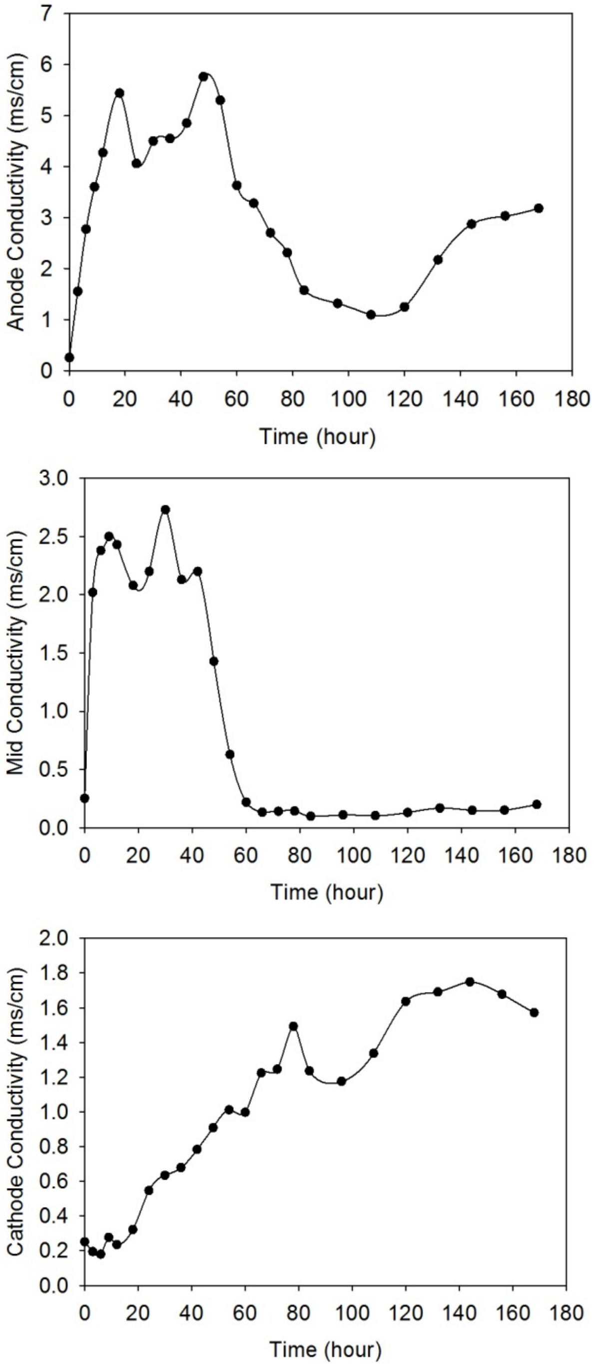

Fig. 6: EC variation in the anode, mid, and cathode compartments versus the time during (EK-1).

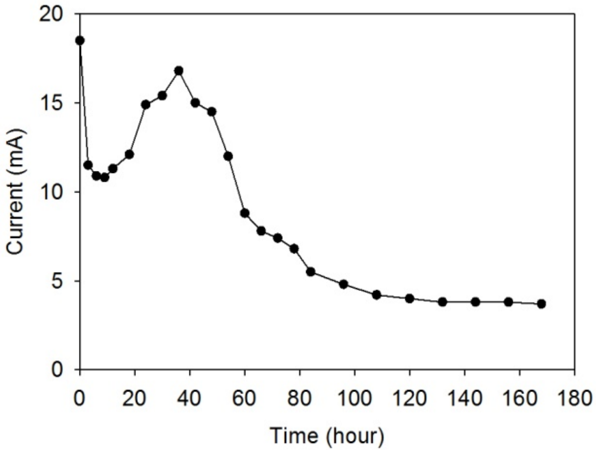

Fig. 7: Current variation versus the time during (EK-1).

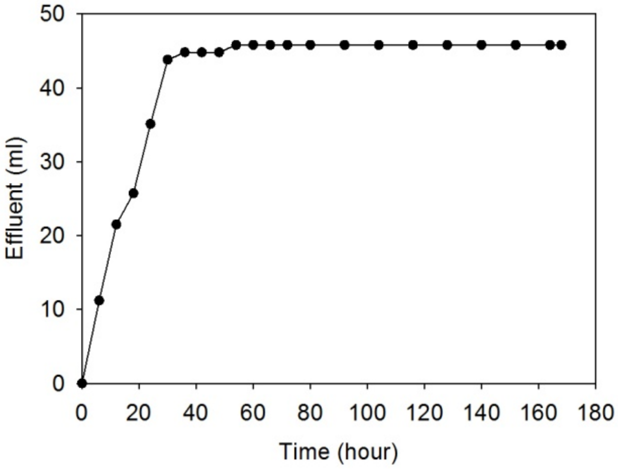

Fig. 8: Effluent variation versus the time during (EK-1).

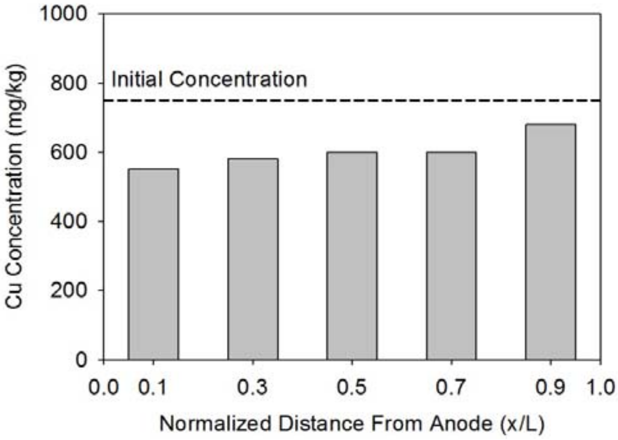

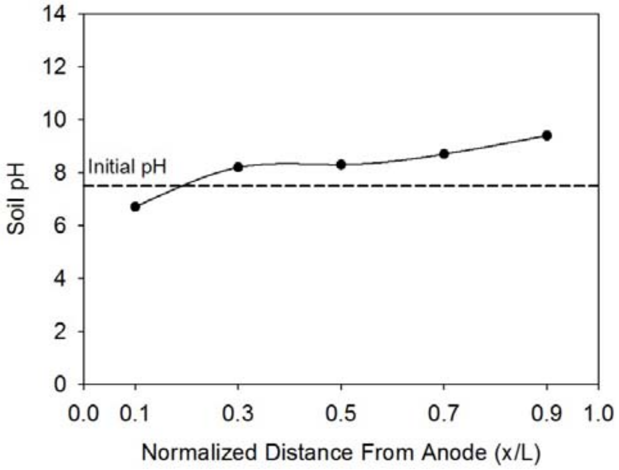

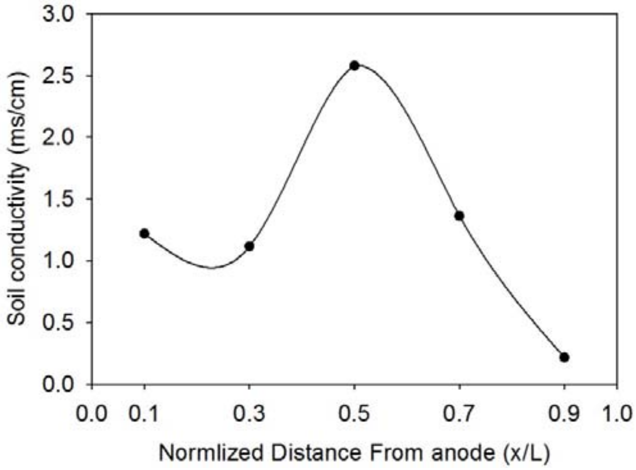

Fig.9: parameters measured after (EK-1) :(a) Cu concentration, (b) pH and (c) EC.

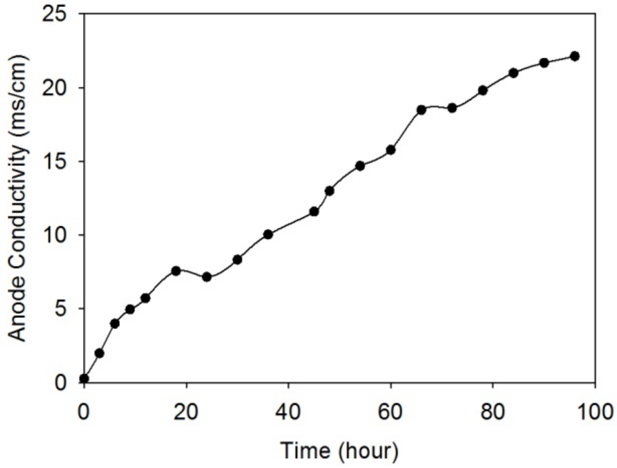

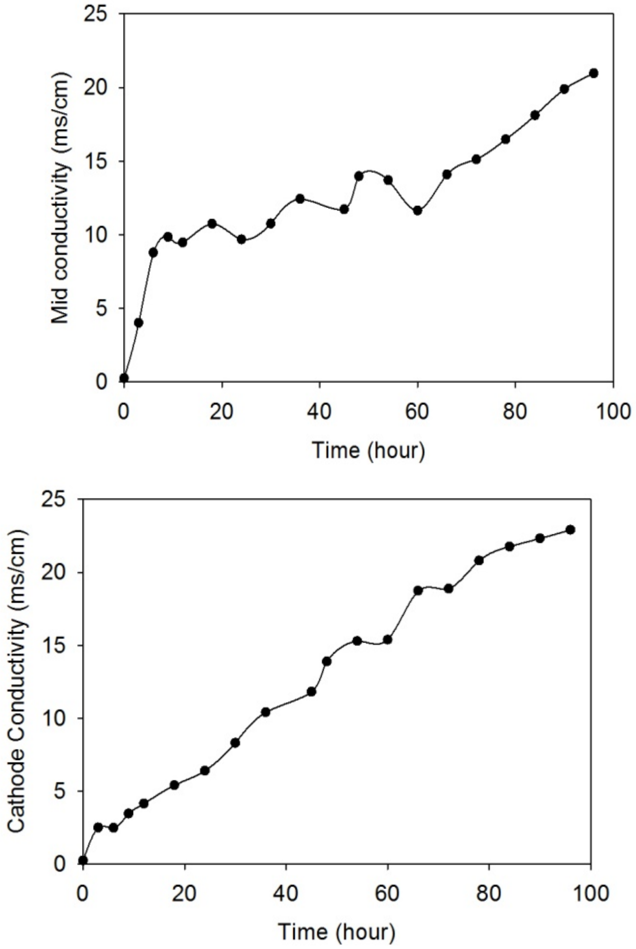

Fig. 10: EC variation in the anode, mid, and cathode compartments versus the time during (EK-2).

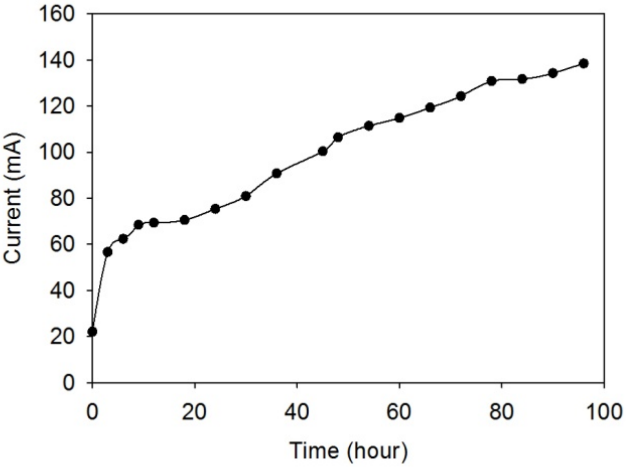

Fig. 11: Current variation versus the time during (EK-2).

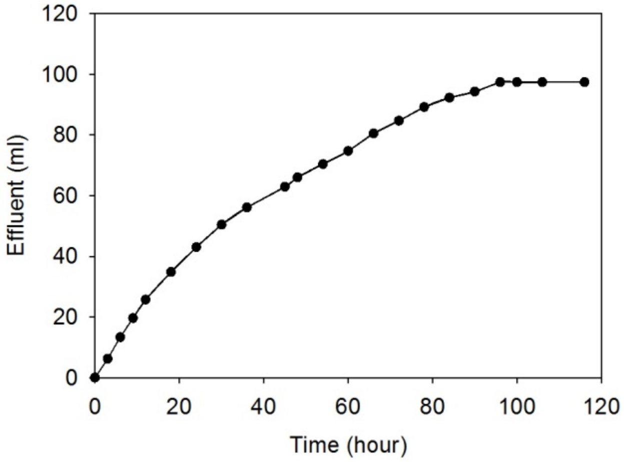

Fig. 12: Effluent variation versus the time during (EK-2).

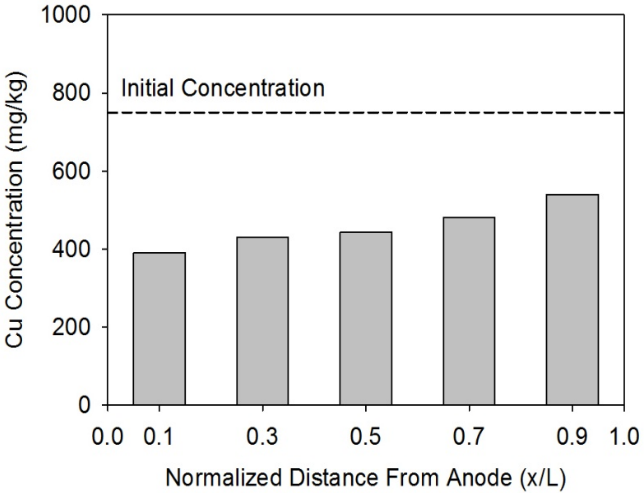

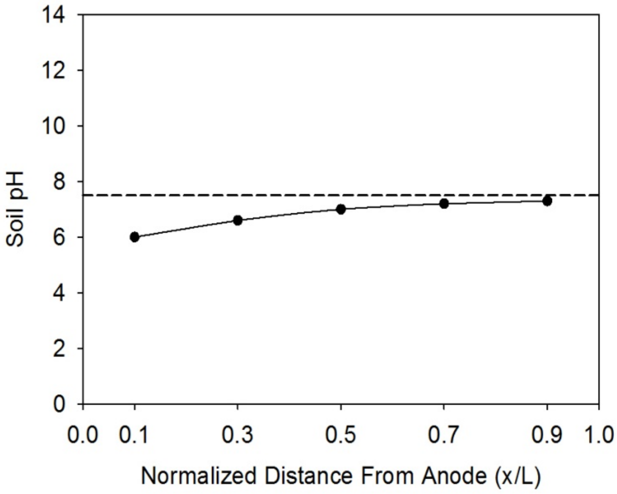

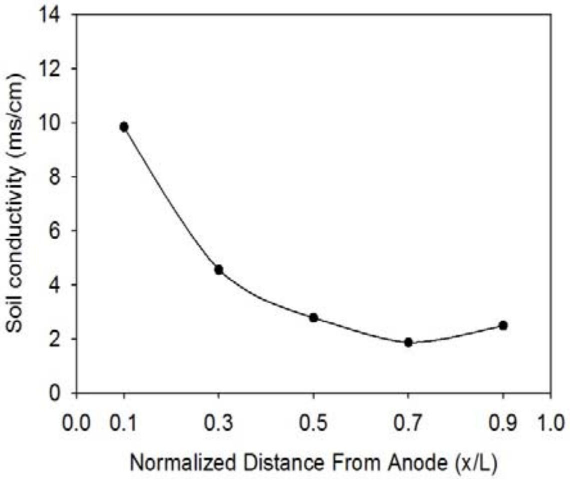

Fig.13: parameters measured after (EK-2) :(a) Cu concentration, (b) pH and (c) EC.

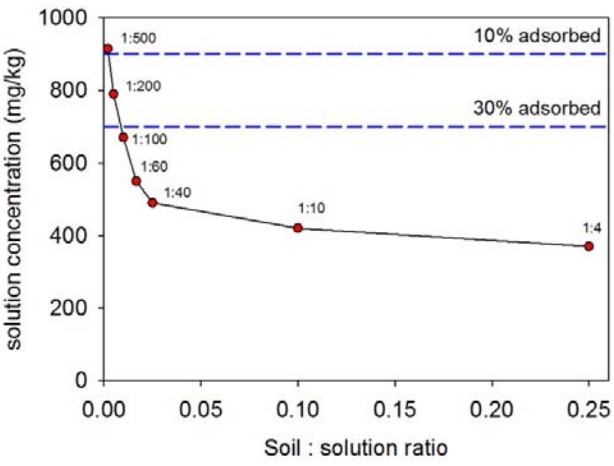

Fig.14: Distribution of copper concentrations after 24 hours of contact time with sandy loam soil as a function of soil: solution ratio at 25°C.

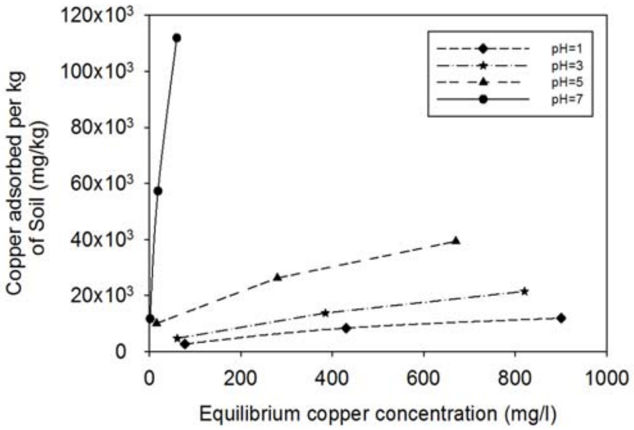

Fig. 15: Adsorption of copper onto sandy loam soil as a function of pH at 25°C.

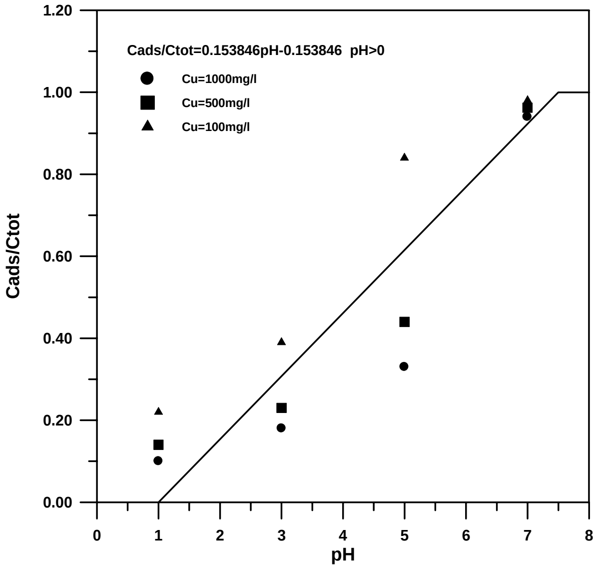

Fig.16: Adsorption isotherm of copper onto sandy loam soil as a function of pH and concentration at 25°C.

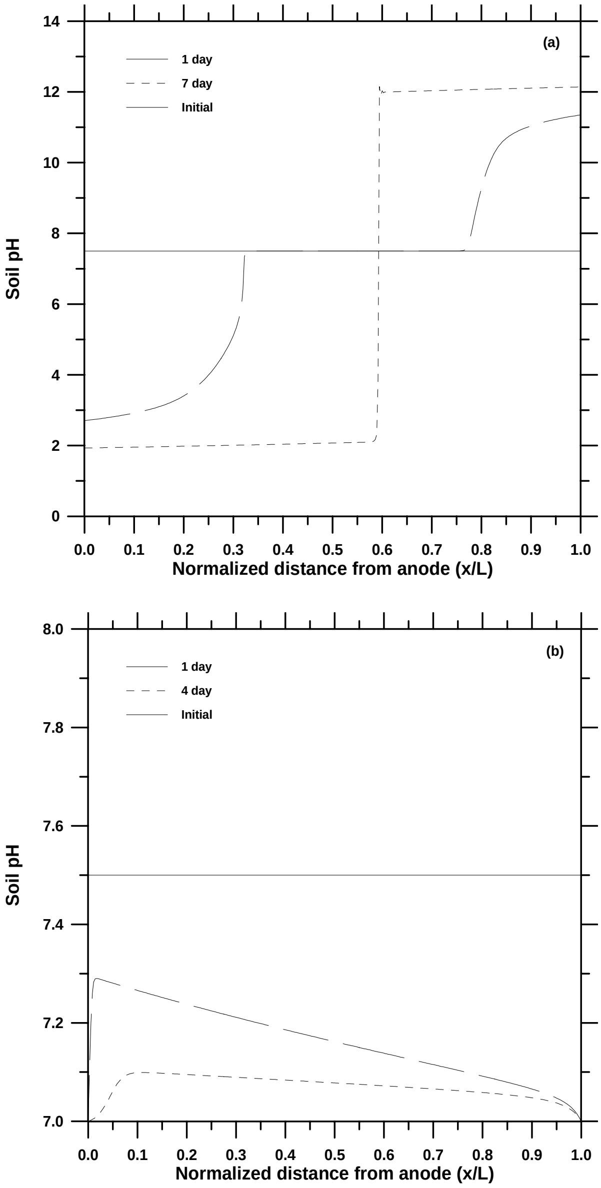

Fig.17: Predicted pH profiles in sandy loam soil: (a) Ek-1; (b) Ek-2.

Table 4: Measured parameters and constants used in the numerical simulation for sandy loam soil.

No.	Parameter	Value
1	Number of species	4
2	Length of soil specimen (m)	0.18
3	Number of nodes	361
4	Time step size (h)	0.01
5	Porosity (n)	0.41*
6	Retardation factor of H^+ (R_H^d)	1.5
7	Bulk density (ρ, kg/m^3)	1272*
8	Tortuosity factor (τ)	0.25
9	Initial soil pH	7.5*
10	Electro-osmotic permeability coefficient (k_{eo}, m^2/Vh)	4.061×10^{-6}*
11	Initial concentration of Cu^{2+} (mg/kg <u>or</u> mol/m^3)	750 <u>or</u> 33.7*
12	Electrical potential (V)	20*

* measured experimentally

Table 5: Effective diffusion coefficients and effective ionic mobilities used in numerical simulation for sandy loam soil.

No.	Species	Diffusion Coefficient (D_i) (m^2/h)	Ionic mobility (u_i) (m^2/Vh)	Effective Diffusion Coefficient (D_i^*) (m^2/h)	Effective Ionic mobility (u_i^*) (m^2/Vh)
1	Cu^{2+}	2.64×10^{-6}	2.05×10^{-4}	2.70×10^{-7}	2.1×10^{-5}
2	H^+	33.52×10^{-6}	13.05×10^{-4}	34.36×10^{-7}	13.38×10^{-5}
3	OH^-	18.97×10^{-6}	7.41×10^{-4}	19.44×10^{-7}	7.59×10^{-5}

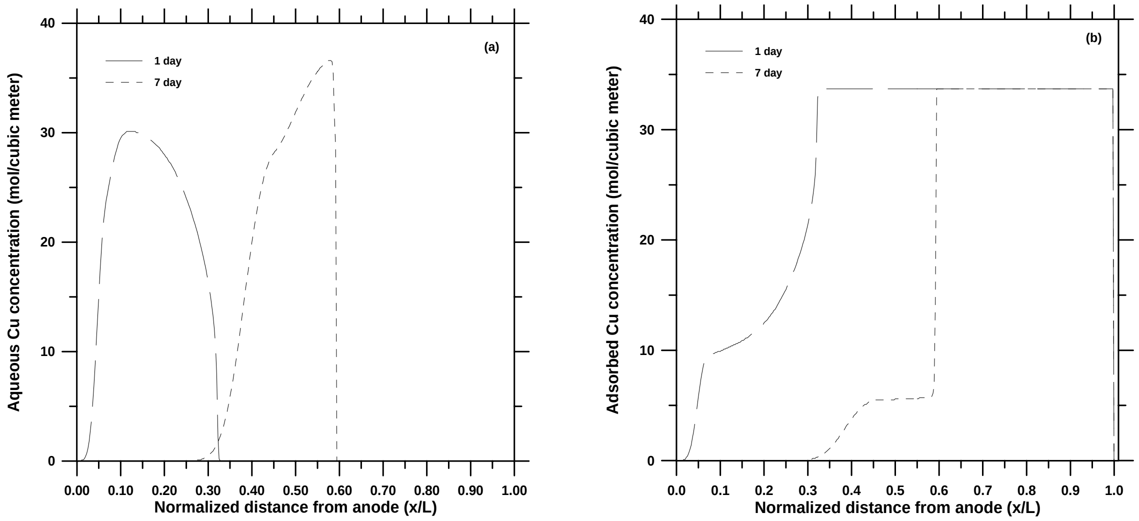

Fig.18: Model predictions of concentration profiles of different forms of Cu^{2+} in the first simulation: (a) aqueous form; (b) adsorbed form.

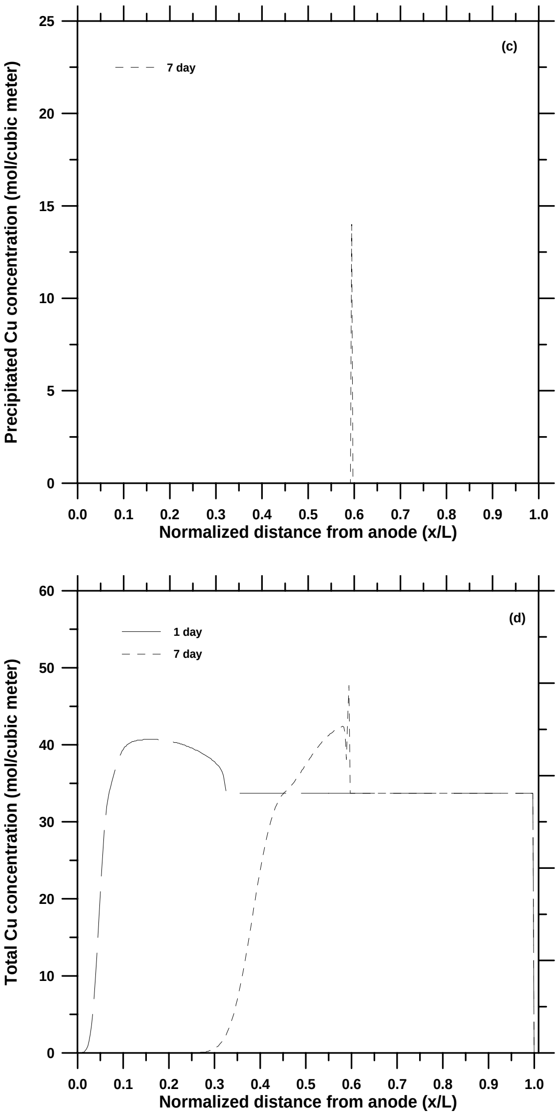

Fig. 18: (c) precipitated form; and (d) total concentration.

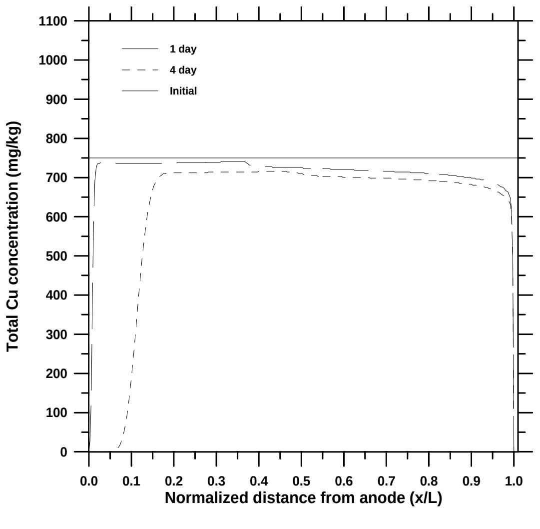

Fig. 19: Model predictions of total Cu^{2+}concentration profile in the second simulation.

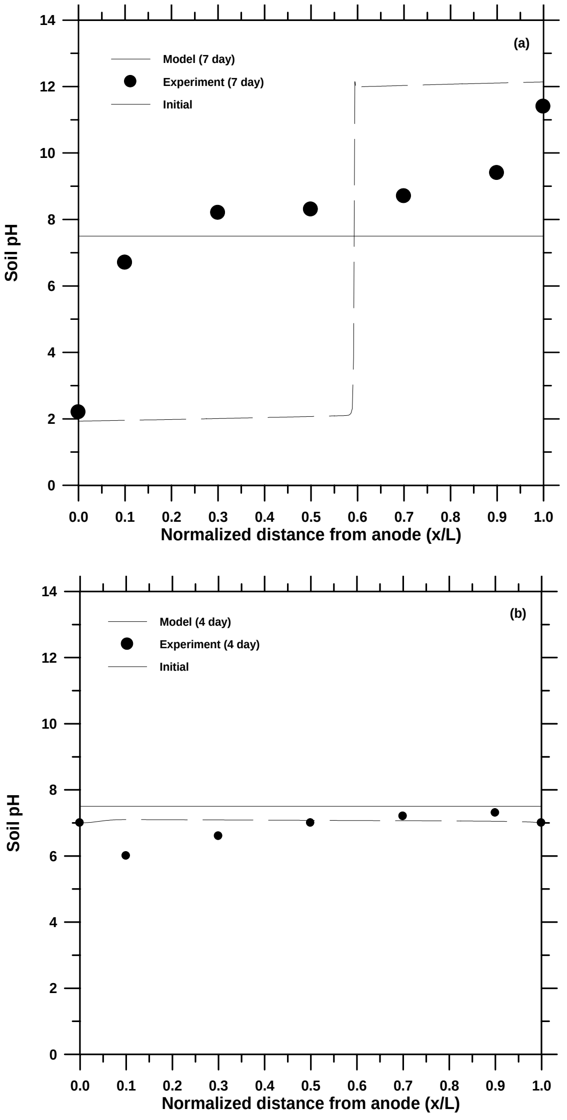

Fig. 20: Comparison between model predictions and experimental results for soil pH profiles in: (a) EK-1 and (b) EK-2.

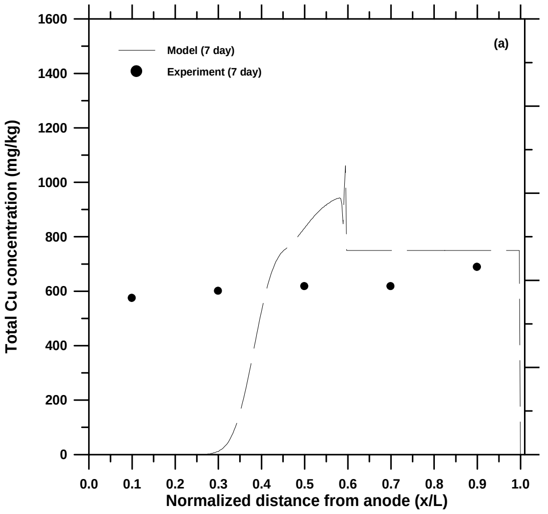

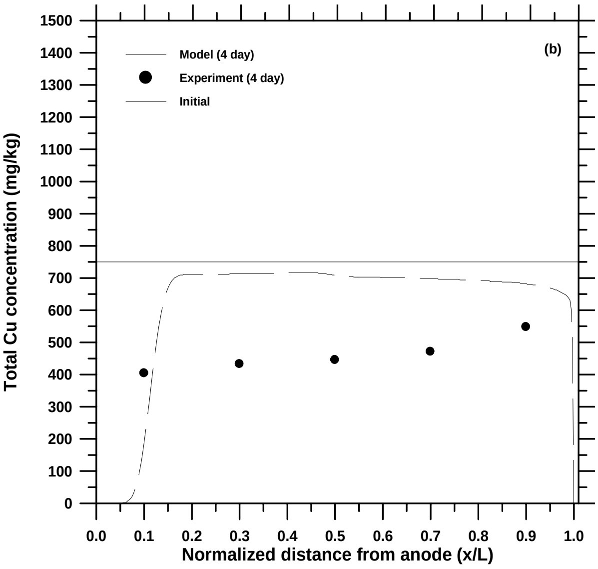

Fig. 21: Comparison between model predictions and experimental results for total Cu^{2+} concentration in soil: (a) EK-1 and (b) EK-2.

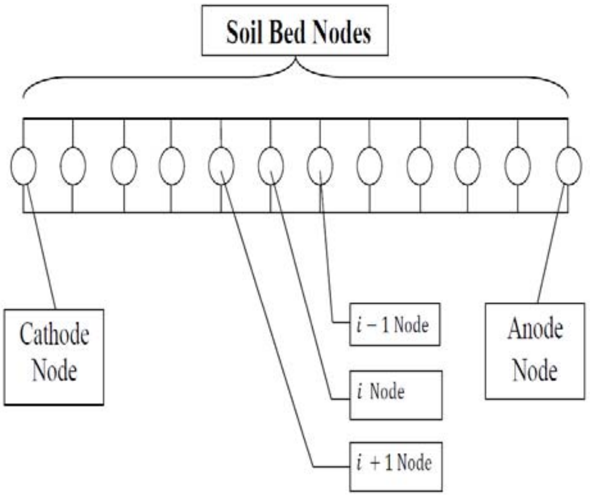

Fig.2: Electro-kinetic cell discretized in a mesh arrangement.

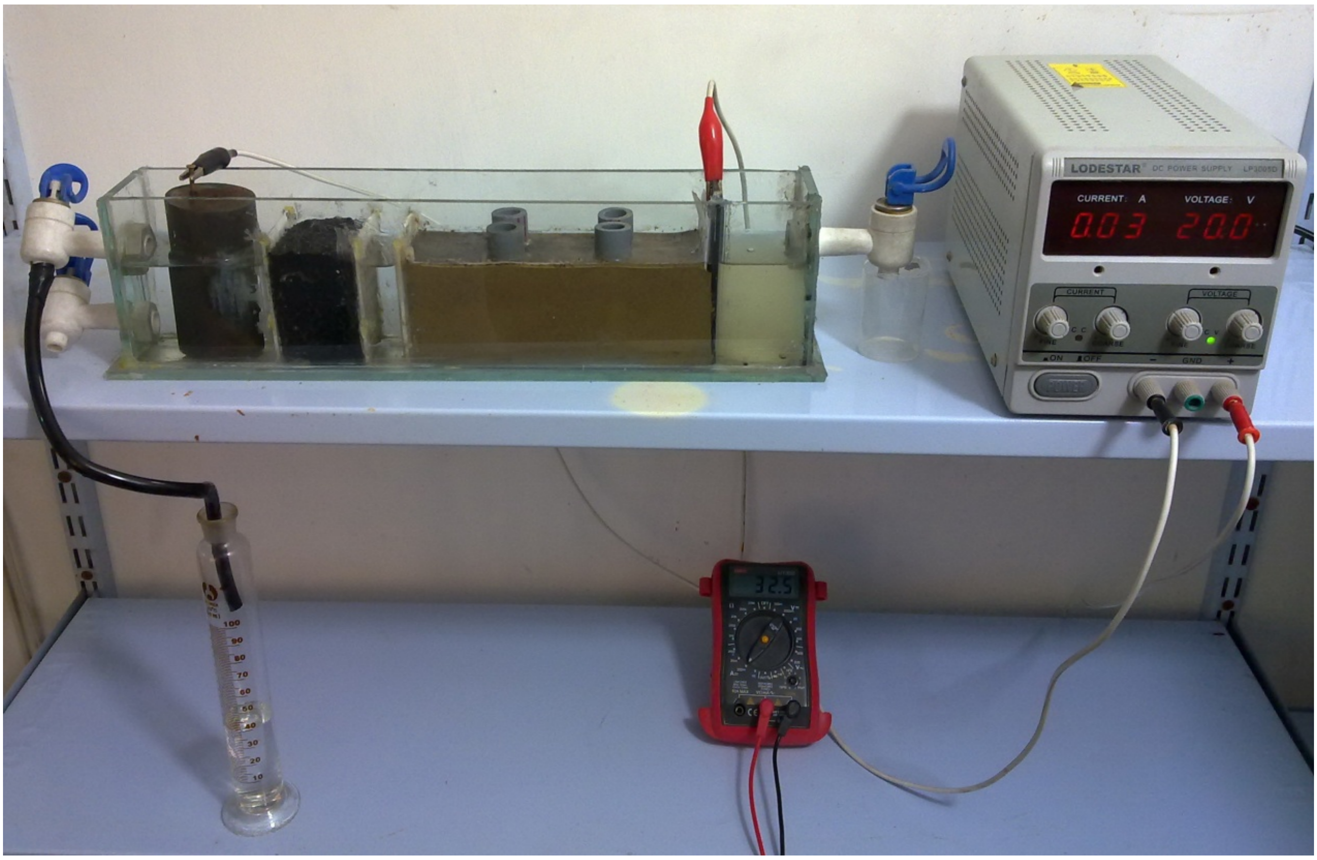

Fig. 22: Experimental set-up of electro-kinetic cell used in the present study.